



NeuroWeaver: An Autonomous Evolutionary Agent for Exploring the Programmatic Space of EEG Analysis Pipelines

Guoan Wang^{1*}, Shihao Yang^{1*}, Jun-En Ding¹, Hao Zhu¹, and Feng Liu^{1**}

Department of Systems Engineering, Stevens Institute of Technology, USA

Abstract. Although foundation models have demonstrated remarkable success in general domains, the application of these models to electroencephalography (EEG) analysis is constrained by substantial data requirements and high parameterization. These factors incur prohibitive computational costs, thereby impeding deployment in resource-constrained clinical environments. Conversely, general-purpose automated machine learning frameworks are often ill-suited for this domain, as exploration within an unbounded programmatic space fails to incorporate essential neurophysiological priors and frequently yields solutions that lack scientific plausibility. To address these limitations, we propose NeuroWeaver, a unified autonomous evolutionary agent designed to generalize across diverse EEG datasets and tasks by reformulating pipeline engineering as a discrete constrained optimization problem. Specifically, we employ a Domain-Informed Subspace Initialization to confine the search to neuroscientifically plausible manifolds, coupled with a Multi-Objective Evolutionary Optimization that dynamically balances performance, novelty, and efficiency via self-reflective refinement. Empirical evaluations across five heterogeneous benchmarks demonstrate that NeuroWeaver synthesizes lightweight solutions that consistently outperform state-of-the-art task-specific methods and achieve performance comparable to large-scale foundation models, despite utilizing significantly fewer parameters.

Keywords: Automated EEG Analysis · Autonomous Evolutionary Agent · Large Language Models (LLMs)

1 Introduction

Electroencephalography (EEG) serves as a pivotal non-invasive modality for decoding complex neural dynamics, providing the high temporal resolution essential for both clinical diagnostics and cognitive analysis [12,3]. However, EEG analysis faces significant challenges due to pronounced data heterogeneity stemming from variations in acquisition hardware, electrode configurations, and subject populations [18]. Although deep learning has demonstrated remarkable suc-

* These authors contributed equally to this work.
 ** Corresponding author: fliu22@stevens.edu

cess in specific tasks, conventional architectures often fail to mitigate these domain shifts effectively [9]. To address this limitation, recent research has gravitated towards foundation models that aim to learn universal representations through large-scale pre-training [19,6]. Nevertheless, this generic approach incurs substantial computational costs and requires extensive datasets that are frequently unavailable in specialized clinical environments. This establishes a fundamental tension between leveraging the generalization capabilities of foundation models and adhering to the strict memory and computational constraints of clinical edge devices, which typically preclude the deployment of resource-intensive architectures.

The integration of Large Language Models (LLMs) into autonomous agents has fundamentally revolutionized automated problem-solving [21,16]. Pioneering frameworks, such as AIDE [7] and ML-Master [11], have demonstrated the efficacy of formulating machine learning engineering as a search problem within the code space. By leveraging tree-structured exploration strategies (e.g., MCTS) alongside iterative refinement policies, these systems autonomously draft, execute, debug, and optimize solution scripts to maximize performance on complex Kaggle machine learning benchmarks. Within the neurophysiological domain, EEGAgent [22] has recently introduced LLM-driven orchestration for EEG analysis. However, this framework functions primarily as a tool-invocation agent rather than an optimization engine. Constrained by the scheduling of static, predefined tools, the approach lacks the capacity for code-level optimization. Moreover, the system is restricted to addressing existing problem formulations and exhibits limited adaptability to novel tasks. Consequently, the field lacks a unified automated agent capable of systematically addressing diverse downstream EEG tasks, including novel ones, by programmatically generating and executing high-performance, lightweight, and task-specific analysis pipelines.

To bridge this gap, we introduce **NeuroWeaver**, an autonomous evolutionary agent that automates the engineering of EEG analysis pipelines by iteratively drafting, debugging, and optimizing programmatic solutions until a multi-objective reward is maximized. As illustrated in Fig. 1a, this agent functions as a unified framework capable of adapting to arbitrary datasets and tasks. It achieves this by synthesizing and optimizing distinct, task-specific code, while autonomously orchestrating the entire lifecycle from model training to result analysis. Our contributions are: (i) We propose the first end-to-end autonomous agent framework tailored for automated EEG pipeline engineering, capable of orchestrating the entire model development lifecycle without human intervention. (ii) We introduce a domain-informed subspace initialization strategy that confines the search space to neuroscientifically plausible manifolds, significantly enhancing both the validity and efficiency of the generated code. (iii) We design a multi-objective reward mechanism that dynamically balances accuracy, novelty, and computational cost, guiding the evolutionary process toward optimal trade-offs between performance and resource efficiency. (iv) Extensive evaluations on five diverse benchmarks demonstrate that NeuroWeaver surpasses state-of-the-art task-specific methods across nearly all metrics with a minimal computa-

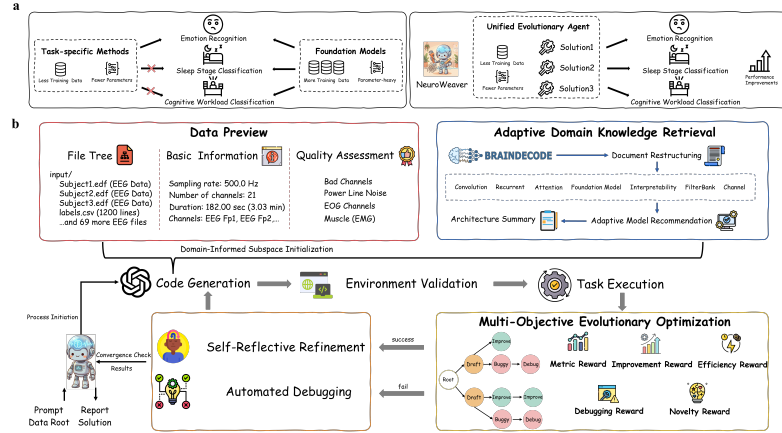


Fig. 1. Framework overview of NeuroWeaver. (a) Paradigm comparison illustrating the transition from static task-specific architectures and resource-intensive foundation models to a unified, adaptive framework that autonomously synthesizes lightweight programmatic solutions. (b) Schematic of the autonomous workflow, detailing the closed-loop optimization cycle that reformulates pipeline engineering as a constrained search process driven by domain-informed subspace initialization and multi-objective evolutionary refinement.

tional footprint, while also outperforming foundation models on the HMC [2] and Workload [24] datasets.

2 Method

2.1 Framework Overview

As depicted in Fig. 1b, upon receiving a task description, evaluation criteria, and the raw data directory, the framework initiates the workflow with Data-Driven Constraint Extraction and Adaptive Domain Knowledge Retrieval. In this phase, the agent identifies intrinsic signal constraints and incorporates relevant neuro-architectural priors to construct a Domain-Informed Subspace Initialization. Conditioned on this restricted manifold, the system leverages generative coding capabilities to synthesize candidate solution scripts. Subsequently, these candidates undergo Environment Validation to address dependency conflicts prior to Task Execution. The resultant performance metrics inform a Multi-Objective Evolutionary Optimization mechanism, which dynamically steers the search trajectory: functional solutions undergo a Self-Reflective Refinement process to balance accuracy with efficiency, whereas erroneous nodes trigger an Automated Debugging routine. This iterative evolution proceeds until convergence criteria are satisfied, yielding an optimal, robust EEG analysis pipeline alongside a comprehensive summary report.

2.2 Problem Formulation

We formulate the automated design of EEG pipelines as a discrete optimization problem within a programmatic space \mathcal{S} . Each candidate solution $s \in \mathcal{S}$ represents an end-to-end executable script, formally defined as a sequential composition of three distinct functional modules:

$$s(x) = (f_{model} \circ f_{pre} \circ f_{load})(x) \quad (1)$$

Specifically, $f_{load}(\cdot)$ manages data ingestion and standardizes heterogeneous raw signals into a unified tensor format; $f_{pre}(\cdot)$ performs signal preprocessing (e.g., spectral filtering and artifact removal) to enhance the signal-to-noise ratio; and $f_{model}(\cdot)$ denotes the learning architecture that maps processed signals to task-specific predictions. The objective is to identify an optimal script s^* that maximizes a composite utility function \mathcal{R} on an unseen test set \mathcal{D}_{test} , subject to the constraint that s maintains executability and logical validity:

$$s^* = \underset{s \in \mathcal{S}}{\operatorname{argmax}} \mathcal{R}(s \mid \mathcal{D}_{test}) \quad (2)$$

This formulation treats code generation not merely as text synthesis, but as a search for a functional mapping within \mathcal{S} that ensures compatibility with the data representations established by f_{load} and f_{pre} .

2.3 Domain-Informed Subspace Initialization

Generic LLMs typically generate code within an unbounded space \mathcal{S} , frequently yielding solutions that are syntactically valid but lack neuroscientific plausibility. To address this challenge, we restrict the search to a domain-specific subspace $\mathcal{S}_{EEG} \subset \mathcal{S}$ through a structured initialization pipeline. This pipeline comprises Data-Driven Constraint Extraction and Adaptive Knowledge Retrieval.

Data-Driven Constraint Extraction. We first employ an automated data preview routine to analyze the raw data directory and construct a metadata descriptor ϕ_{data} . We formalize this process as the extraction of a physical constraint vector rather than simple file reading:

$$\phi_{data} = \langle \mathbf{i}_{EEG}, \mathbf{q}_{artifact} \rangle \quad (3)$$

Here, \mathbf{i}_{EEG} encapsulates intrinsic EEG attributes (e.g., sampling rate and channel layout), while $\mathbf{q}_{artifact}$ quantifies signal quality, including powerline noise levels, EOG artifacts, and EMG contamination ratios. This constraint vector explicitly guides the generation of preprocessing strategies, such as notch filtering and ocular artifact removal, and aligns the input configuration of the model with data specifications. Crucially, this mechanism prevents discrepancies between input and architecture (e.g., inconsistencies in channel counts) that are typical in generic code generation.

Adaptive Knowledge Retrieval. To incorporate neuro-architectural priors, we design a two-stage retrieval mechanism leveraging Braindecode [14], an open-source library for deep learning analysis of EEG signals. First, given the objective

of the downstream task T_{goal} , the retrieval module queries the library. Adhering to the official taxonomy of Braindecode (e.g., Convolution, Attention, and Recurrent), the system selects one representative model m_c for each category $c \in \mathcal{C}_{BD}$ to instantiate a candidate set $\mathcal{M}_{cand} = \{m_c \mid c \in \mathcal{C}_{BD}\}$. Second, to bridge the semantic gap between complex source code and LLM comprehension, a summarization function parses the source code and documentation associated with \mathcal{M}_{cand} . This function distills the technical details into a concise textual summary of architectural features, denoted as \mathcal{T}_{prior} .

Initialization of the Search Subspace. Consequently, the optimization problem is constrained by these distinct modalities. The agent generates the initial root solution s_0 via a conditional mapping rather than random initialization:

$$s_0 = \pi_\theta(s \mid T_{goal}, \phi_{data}, \mathcal{T}_{prior}) \quad (4)$$

By conditioning the generative policy π_θ on the data constraints ϕ_{data} and the textual architectural priors \mathcal{T}_{prior} , the agent is constrained to generate solutions within a neuroscientifically plausible manifold \mathcal{S}_{EEG} . This restriction prunes the search space prior to the commencement of the iterative process.

2.4 Multi-Objective Evolutionary Optimization

To effectively navigate the complex programmatic space of EEG analysis, we formulate the pipeline engineering process as a tree-structured search, leveraging the exploration paradigm established in ML-Master [11]. In contrast to sequential code generation, this framework maintains a solution tree in which each node represents a fully executable pipeline script, and edges denote evolutionary steps—specifically, iterative code modifications conditioned on execution feedback.

The optimization process operates as a closed-loop cycle. Following the execution of a candidate solution s_t , the system evaluates the execution outcomes to determine the direction of the subsequent iteration. This decision-making process is governed by a feedback mechanism, in which a semantic diagnosis module synthesizes the architectural logic and performance metrics of the parent node into actionable refinement instructions. These instructions subsequently guide the generation of a child node s_{t+1} , with the objective of rectifying theoretical flaws or optimizing the hyperparameters of the parent node s_t .

To mitigate convergence to suboptimal local minima and ensure strict alignment with the objectives of the system, we regulate this evolutionary process through a multi-objective reward mechanism. Following execution, this mechanism assigns a scalar score to each generated node, serving as the primary criterion for guiding subsequent expansions. Formally, the composite reward $R(s)$ for a candidate solution s is defined as:

$$R(s) = w_m \mathcal{M}(s|\mathcal{D}) + w_i \Delta(s, s_{parent}) + w_n \Omega(s) + w_e \Gamma(\tau_s) + w_{fix} \Phi(s) \quad (5)$$

In this formulation, the coefficients $w_m, w_i, w_n, w_e, w_{fix}$ regulate the trade-off among competing objectives. The term $\mathcal{M}(s|\mathcal{D})$ denotes the primary performance metric (e.g., Balanced Accuracy) evaluated on the target dataset. To

Table 1. Performance comparison on SEED and HMC datasets.

Method	Model Size	SEED			HMC		
		Balanced Acc.	Cohen's Kappa	Weighted F1	Balanced Acc.	Cohen's Kappa	Weighted F1
<i>Task-specific Methods</i>							
SPaRCNet [8]	0.79M	0.5596 \pm 0.0244	0.3464 \pm 0.0372	0.5585 \pm 0.0297	0.4756 \pm 0.1109	0.3147 \pm 0.1315	0.4108 \pm 0.1310
ContraWR [20]	1.6M	0.6106 \pm 0.0078	0.4220 \pm 0.0129	0.6137 \pm 0.0085	0.4242 \pm 0.0541	0.2340 \pm 0.0554	0.2987 \pm 0.0288
CNN-Transformer [13]	3.2M	0.6161 \pm 0.0384	0.4262 \pm 0.0601	0.6150 \pm 0.0463	0.6573 \pm 0.0141	0.5961 \pm 0.0105	0.6896 \pm 0.0065
FFCL [10]	2.4M	0.5808 \pm 0.0322	0.3732 \pm 0.0462	0.5743 \pm 0.0402	0.4427 \pm 0.0702	0.2542 \pm 0.0654	0.2902 \pm 0.0485
ST-Transformer [15]	3.5M	0.5479 \pm 0.0091	0.3261 \pm 0.0169	0.5505 \pm 0.0091	0.2559 \pm 0.0141	0.0503 \pm 0.0183	0.1428 \pm 0.0122
<i>Pretrained Foundation Models</i>							
BIOT [19]	3.2M	0.7097 \pm 0.0024	0.5682 \pm 0.0051	0.7134 \pm 0.0027	0.6862 \pm 0.0041	0.6295 \pm 0.0113	0.7091 \pm 0.0147
LaBraM-Base [6]	5.8M	0.7318 \pm 0.0019	0.5994 \pm 0.0031	0.7354 \pm 0.0021	0.7286 \pm 0.0101	0.6812 \pm 0.0073	0.7554 \pm 0.0024
NeuroLM-B [5]	254M	0.5554 \pm 0.0075	0.3393 \pm 0.0117	0.5599 \pm 0.0068	0.6737 \pm 0.0050	0.6188 \pm 0.0057	0.7126 \pm 0.0034
<i>Agent System</i>							
NeuroWeaver	0.37M/0.18M	0.6211 \pm 0.0058	0.4397 \pm 0.0087	0.6246 \pm 0.0058	0.7737 \pm 0.0079	0.6934 \pm 0.0128	0.7630 \pm 0.0123

promote substantial performance gains, $\Delta(s, s_{parent})$ quantifies the incremental improvement of the current node relative to its direct parent. Diversity is maintained via a novelty estimation function $\Omega(s)$, which leverages the semantic reasoning capabilities of a LLMs to conduct a contrastive analysis against the archive of historical solutions, thereby penalizing redundancy. Computational efficiency is quantified by $\Gamma(\tau_s) = 1 - \sqrt{\min(1, \tau_s/\tau_{max})}$, where τ_s represents the execution latency of the solution s , thereby penalizing pipelines that exceed the temporal budget τ_{max} . Finally, to ensure code robustness, we incorporate a debugging reward $\Phi(s)$ that evaluates the executability and syntactic validity of the script, imposing penalties on runtime failures to guide the evolution toward functional solutions.

3 Experiments

Experimental Setup. To ensure rigorous and fair comparison with state-of-the-art methods, we align our protocols with NeuroLM [5]. We evaluate NeuroWeaver on five heterogeneous benchmarks—TUEV [4], SEED [23], HMC [2], Workload [24], and TUSL [17]—encompassing diverse cognitive and physiological tasks. To prevent leakage, data partitioning follows the subject-independent, chronological, or random strategies defined by the baselines. Preprocessing is standardized for consistency: raw EEG signals undergo 0.1–75 Hz bandpass filtering, region-adaptive notch filtering (50/60 Hz), temporal resampling to 200 Hz, and global amplitude scaling by 10^{-2} . While initial preprocessing is fixed, we impose no constraints on subsequent processing. We quantify performance primarily using Balanced Accuracy, employing AUROC and AUPRC for binary classification, and Cohen κ and Weighted F1-score for multi-class tasks. The framework utilizes ChatGPT-5.1 [1] as the unified backbone. Evolutionary optimization operates with a global budget of 200 iterations and parallelism of 3, incurring an approximate API cost of \$20 USD per individual run.

Comparative Analysis. We evaluate the performance of NeuroWeaver against state-of-the-art task-specific methods [8,20,13,10,15] and large-scale pretrained foundation models [19,6,5] across five diverse EEG datasets (Tables 1, 2, and 3).

Table 2. Performance comparison on TUEV and TUSL datasets.

Method	Model Size	TUEV			TUSL		
		Balanced Acc.	Cohen's Kappa	Weighted F1	Balanced Acc.	Cohen's Kappa	Weighted F1
<i>Task-specific Methods</i>							
SPaRCNet [8]	0.79M	0.4161 \pm 0.0262	0.4233 \pm 0.0181	0.7024 \pm 0.0104	0.4185 \pm 0.0452	0.1399 \pm 0.0799	0.3500 \pm 0.0968
ContraWR [20]	1.6M	<u>0.4384</u> \pm 0.0349	0.3912 \pm 0.0237	0.6893 \pm 0.0136	<u>0.5857</u> \pm 0.0662	<u>0.3567</u> \pm 0.0968	<u>0.5458</u> \pm 0.0798
CNN-Transformer [13]	3.2M	0.4087 \pm 0.0161	0.3815 \pm 0.0134	0.6854 \pm 0.0293	0.3575 \pm 0.0151	0.0306 \pm 0.0179	0.2235 \pm 0.0251
FFCL [10]	2.4M	0.3979 \pm 0.0104	0.3732 \pm 0.0181	0.6783 \pm 0.0120	0.3819 \pm 0.0688	0.0628 \pm 0.0888	0.2120 \pm 0.0786
ST-Transformer [15]	3.5M	0.3984 \pm 0.0228	0.3765 \pm 0.0301	0.6823 \pm 0.0190	0.4000 \pm 0.0329	0.0860 \pm 0.0449	0.3793 \pm 0.0459
<i>Pretrained Foundation Models</i>							
BIOT [19]	3.2M	0.5281 \pm 0.0225	0.5273 \pm 0.0249	0.7492 \pm 0.0082	0.5758 \pm 0.0303	0.2012 \pm 0.0212	0.2394 \pm 0.0040
LaBraM-Base [6]	5.8M	<u>0.6409</u> \pm 0.0065	<u>0.6637</u> \pm 0.0093	<u>0.8312</u> \pm 0.0052	<u>0.7625</u> \pm 0.0131	<u>0.6407</u> \pm 0.0304	<u>0.7614</u> \pm 0.0210
NeuroLM-B [5]	254M	0.4560 \pm 0.0048	0.4285 \pm 0.0048	0.7153 \pm 0.0028	0.6734 \pm 0.0436	0.5107 \pm 0.0617	0.6743 \pm 0.0394
<i>Agent System</i>							
NeuroWeaver	1.2M/0.46M	0.4573 \pm 0.0231	0.4562 \pm 0.0148	0.7285 \pm 0.0110	0.5859 \pm 0.0101	0.1449 \pm 0.0240	0.3742 \pm 0.0311

Table 3. Performance comparison on Workload datasets.

Method	Model Size	Workload		
		Balanced Acc.	AUC-PR	AUROC
<i>Task-specific Methods</i>				
SPaRCNet [8]	0.79M	0.5977 \pm 0.0071	0.6638 \pm 0.0314	0.6717 \pm 0.0172
ContraWR [20]	1.6M	0.6966 \pm 0.0332	0.7668 \pm 0.0408	0.7685 \pm 0.0317
CNN-Transformer [13]	3.2M	0.5793 \pm 0.0230	0.5306 \pm 0.0459	0.5663 \pm 0.0349
FFCL [10]	2.4M	<u>0.7069</u> \pm 0.0197	<u>0.7823</u> \pm 0.0099	<u>0.7357</u> \pm 0.0234
ST-Transformer [15]	3.5M	0.6103 \pm 0.0056	0.5716 \pm 0.0071	0.6375 \pm 0.0078
<i>Pretrained Foundation Models</i>				
BIOT [19]	3.2M	0.6655 \pm 0.0665	0.7189 \pm 0.0722	0.7342 \pm 0.0536
LaBraM-Base [6]	5.8M	0.6609 \pm 0.0204	0.7174 \pm 0.0234	0.7272 \pm 0.0165
NeuroLM-B [5]	254M	0.6172 \pm 0.0113	0.5824 \pm 0.0080	0.6253 \pm 0.0160
<i>Agent System</i>				
NeuroWeaver	0.011M	0.7391 \pm 0.0439	0.8436 \pm 0.0373	0.8403 \pm 0.0361

To ensure statistical reliability, we select the optimal synthesized pipeline s^* for each benchmark and report the mean and standard deviation across **three** independent trials, utilizing distinct **random seeds** where supported by the generated programmatic logic. Underlined entries denote the best performance per category, while **blue** text highlights NeuroWeaver outperforming the leading task-specific baseline; dual model sizes correspond to the left and right datasets, respectively. Empirical results demonstrate that the agent-synthesized pipelines consistently surpass task-specific baselines across nearly all evaluation metrics, while maintaining a substantially smaller parameter count. NeuroWeaver also outperforms resource-intensive foundation models on the HMC [2] and Workload [24] benchmarks, thereby validating the capability of the system to autonomously derive lightweight and high-performance solutions.

Optimization Trajectory. To empirically validate the effectiveness of the closed-loop refinement mechanism, we visualize the performance trajectory of the lineage of the optimal solution. We track the step-wise progression of Balanced Accuracy from the initial root candidate (s_0) to the global optimum (s^*) across all benchmarks. As illustrated in Fig. 2, the results exhibit a consistent performance improvement as the search depth increases. Complementing these quantitative metrics, the bottom-right panel presents a representative solution tree for the HMC [2] dataset, visualizing the topological structure of the evolutionary exploration within the programmatic space.

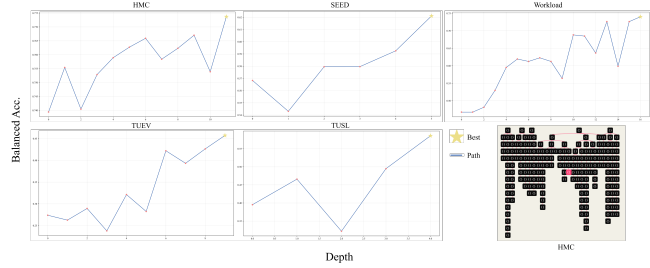


Fig. 2. Optimization trajectory and representative evolutionary solution tree topology.

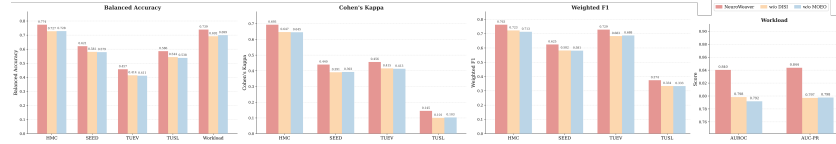


Fig. 3. Quantitative results of the ablation study.

Ablation Study. To evaluate the efficacy of each individual component, we conduct an ablation study by excluding the Domain-Informed Subspace Initialization (w/o DISI) and the Multi-Objective Evolutionary Optimization (w/o MOEO). As demonstrated in Fig. 3, the substantial performance degradation observed in these variants underscores the necessity of incorporating both the domain-constrained initialization and the evolutionary search strategy to synthesize optimal pipelines.

4 Discussion & Conclusion

We introduce NeuroWeaver, establishing a unified paradigm for automatically synthesizing analysis pipelines across diverse EEG datasets and downstream tasks. While standardized preprocessing ensured fair comparisons, this constraint inevitably limited the optimization landscape. Relaxing these restrictions to facilitate holistic pipeline evolution (from signal cleaning to inference) offers potential for superior performance in unconstrained applications. Crucially, the framework strictly adheres to data privacy and security standards by architecturally decoupling semantic reasoning from data execution. Specifically, LLMs interact exclusively with desensitized metadata (e.g., channel configurations, sampling rates, and task descriptions) rather than raw electrophysiological signals. Pipeline synthesis is performed remotely, while generated code execution is strictly confined to the user’s local runtime environment. This design ensures privacy-sensitive EEG recordings remain within local infrastructure, eliminating data leakage risks during interactions with external models.

References

1. Achiam, J., Adler, S., Agarwal, S., Ahmad, L., Akkaya, I., Aleman, F.L., Almeida, D., Altenschmidt, J., Altman, S., Anadkat, S., et al.: Gpt-4 technical report. arXiv preprint arXiv:2303.08774 (2023)
2. Alvarez-Estevez, D., Rijsman, R.M.: Inter-database validation of a deep learning approach for automatic sleep scoring. *PloS One* **16**(8), e0256111 (2021)
3. Cohen, M.X.: *Analyzing neural time series data: theory and practice*. MIT press (2014)
4. Harati, A., Golmohammadi, M., Lopez, S., Obeid, I., Picone, J.: Improved EEG event classification using differential energy. In: 2015 IEEE Signal Processing in Medicine and Biology Symposium (SPMB). pp. 1–4. IEEE (2015)
5. Jiang, W.B., Wang, Y., Lu, B.L., Li, D.: Neurolm: A universal multi-task foundation model for bridging the gap between language and eeg signals. arXiv preprint arXiv:2409.00101 (2024)
6. Jiang, W.B., Zhao, L.M., Lu, B.L.: Large brain model for learning generic representations with tremendous eeg data in bci. arXiv preprint arXiv:2405.18765 (2024)
7. Jiang, Z., Schmidt, D., Srikanth, D., Xu, D., Kaplan, I., Jacenko, D., Wu, Y.: Aide: Ai-driven exploration in the space of code. arXiv preprint arXiv:2502.13138 (2025)
8. Jing, J., Ge, W., Hong, S., Fernandes, M.B., Lin, Z., Yang, C., An, S., Struck, A.F., Herlopian, A., Karakis, I., et al.: Development of expert-level classification of seizures and rhythmic and periodic patterns during EEG interpretation. *Neurology* **100**(17), e1750–e1762 (2023)
9. Lawhern, V.J., Solon, A.J., Waytowich, N.R., Gordon, S.M., Hung, C.P., Lance, B.J.: Eegnet: a compact convolutional neural network for eeg-based brain–computer interfaces. *Journal of neural engineering* **15**(5), 056013 (2018)
10. Li, H., Ding, M., Zhang, R., Xiu, C.: Motor imagery EEG classification algorithm based on CNN-LSTM feature fusion network. *Biomedical Signal Processing and Control* **72**, 103342 (2022)
11. Liu, Z., Cai, Y., Zhu, X., Zheng, Y., Chen, R., Wen, Y., Wang, Y., Chen, S., et al.: Ml-master: Towards ai-for-ai via integration of exploration and reasoning. arXiv preprint arXiv:2506.16499 (2025)
12. Niedermeyer, E., da Silva, F.L.: *Electroencephalography: basic principles, clinical applications, and related fields*. Lippincott Williams & Wilkins (2005)
13. Peh, W.Y., Yao, Y., Dauwels, J.: Transformer convolutional neural networks for automated artifact detection in scalp EEG. In: 2022 44th Annual International Conference of the IEEE Engineering in Medicine & Biology Society (EMBC). pp. 3599–3602. IEEE (2022)
14. Schirrmeister, R.T., Springenberg, J.T., Fiederer, L.D.J., Glasstetter, M., Eggensperger, K., Tangermann, M., Hutter, F., Burgard, W., Ball, T.: Deep learning with convolutional neural networks for eeg decoding and visualization. *Human Brain Mapping* (aug 2017). <https://doi.org/10.1002/hbm.23730>, <http://dx.doi.org/10.1002/hbm.23730>
15. Song, Y., Jia, X., Yang, L., Xie, L.: Transformer-based spatial-temporal feature learning for EEG decoding. arXiv preprint arXiv:2106.11170 (2021)
16. Wang, L., Ma, C., Feng, X., Zhang, Z., Yang, H., Zhang, J., Chen, Z., Tang, J., Chen, X., Lin, Y., et al.: A survey on large language model based autonomous agents. *Frontiers of Computer Science* **18**(6), 186345 (2024)

17. von Weltin, E., Ahsan, T., Shah, V., Jamshed, D., Golmohammadi, M., Obeid, I., Picone, J.: Electroencephalographic slowing: A primary source of error in automatic seizure detection. In: 2017 IEEE Signal Processing in Medicine and Biology Symposium (SPMB). pp. 1–5. IEEE (2017)
18. Xu, L., Xu, M., Ke, Y., An, X., Liu, S., Ming, D.: Cross-dataset variability problem in eeg decoding with deep learning. *Frontiers in human neuroscience* **14**, 103 (2020)
19. Yang, C., Westover, M., Sun, J.: Biot: Biosignal transformer for cross-data learning in the wild. *Advances in Neural Information Processing Systems* **36**, 78240–78260 (2023)
20. Yang, C., Xiao, C., Westover, M.B., Sun, J.: Self-supervised electroencephalogram representation learning for automatic sleep staging: model development and evaluation study. *JMIR AI* **2**(1), e46769 (2023)
21. Yao, S., Zhao, J., Yu, D., Du, N., Shafran, I., Narasimhan, K.R., Cao, Y.: React: Synergizing reasoning and acting in language models. In: The eleventh international conference on learning representations (2022)
22. Zhao, S., Peng, M., Jiang, H., Li, T., Li, S., Pan, G.: Eegagent: A unified framework for automated eeg analysis using large language models. *arXiv preprint arXiv:2511.09947* (2025)
23. Zheng, W.L., Lu, B.L.: Investigating critical frequency bands and channels for EEG-based emotion recognition with deep neural networks. *IEEE Transactions on Autonomous Mental Development* **7**(3), 162–175 (2015)
24. Zyma, I., Tukaev, S., Seleznov, I., Kiyono, K., Popov, A., Chernykh, M., Shpenkov, O.: Electroencephalograms during mental arithmetic task performance. *Data* **4**(1), 14 (2019)